PHYSICAL REVIEW VOLUME 111, NUMBER 1 JULY 1, 1958

Electrical Conduction via Slow Surface States on Semiconductors

H. Statz and G. A. deMars
Research Division, Raytheon Manufacturing Company, Waltham, Massachusetts

(Received January 6, 1958; revised manuscript received May 1, 1958)

Steady-state and transient conductance of inversion layers created by acetone vapor on silicon *n-p-n* bars were investigated. The interpretation gives strong evidence that the charge in the outer surface states can move in an electric field. The mobility of the charge is found to be of the order of 10^{-3} cm^2/volt sec for thick films. The mobility becomes progressively smaller in thinner films. It is found that inversion layers created by mobile charges may be unstable for certain applied voltages—in which case large potential jumps occur where the inversion layer meets the main *p-n* junction. It is shown that in many cases the inversion layer current is multiplied while flowing through this potential jump. Possible multiplication mechanisms will be discussed.

INTRODUCTION

A GREAT amount of work has been done to clarify the surface properties of semiconductors. From these investigations one knows that there are various sets of electronic levels in the forbidden gap which are located at the interface between the semiconductor and the oxide film and that there are other surface states with a greater density on the surface of the oxide film. The interface states can communicate well with both the conduction and valence bands and thus act as surface recombination centers. The surface states on the surface of the oxide film can only slowly exchange electrons with the semiconductor. Deviations from their equilibrium occupation decrease with a time constant varying from a fraction of a second to a few hours, depending upon the thickness and structure of the oxide film. In recent work a relatively good understanding of the properties of the interface states[1–4] has been obtained. The properties of the outer surface states are not as well known. In particular, outer surface states produced by thick adsorbed layers of certain liquids present major problems.

It has long been realized[5–8] that water vapor and certain other vapors produce effects on diodes and transistors that are not understandable with the present surface model. These effects include the anomalously high reverse currents of diodes, the reverse current-voltage characteristic which is far from the logarithmic law predicted by inversion layer theory, and the many types of transient currents after a sudden application of a reverse bias.

Eriksen, together with the authors,[8] studied some of these effects. The investigations showed conclusively that conventional ionic conduction could not account for the observations. It was further concluded that electrical conduction through holes in the liquid film might be responsible for the observed currents. In the present paper the same problem has been further investigated. It will be shown that indeed the charge in the outer surface states can move, confirming some earlier postulates.[8,9] However, the detailed processes are more complicated than had been anticipated earlier. It will be shown that the mobility of the charge in the outer surface states is rather low and, in general, does not exceed 10^{-3} cm^2/volt sec. The direct contribution of the current carried by the outer surface states is always negligible as compared to the current carried by the inversion layer. In the previous investigation[8] this fact was not recognized and it was thought possible that the current in the liquid could dominate over the inversion layer current. Effects due to charge movement become observable when there are electric fields parallel to the surface. Such electric fields can be produced, for example, by current flow in inversion layers biased in reverse with respect to the underlying semiconductor material. The charge movement, in general, creates regions in which there is an excess or a deficiency of surface charge density with respect to the density present under equilibrium conditions. Since the inversion layer conductance is a function of the surface charge density, similar variations in the conductance of the inversion layer are found. In regions where the conductance has decreased, the inversion layer current will produce larger tangential field strengths and more charge will flow away. Eventually, there may no longer be enough charge to support an inversion layer. Situations like this are found where inversion layers meet bulk junctions and it will be shown that this process is important to explain many transient phenomena and diode characteristics. Also, in these cases large electric field strengths are produced where the inversion layer meets the bulk junction. The inversion layer current flowing through this high field region may be multiplied at total applied voltages which are smaller than those required for bulk breakdown. Possible breakdown mechanisms will be discussed.

The reported measurements are more complete and more conclusive than the early investigations[8] because

---

[1] Statz, deMars, Davis, and Adams, Phys. Rev. **106**, 455 (1957).
[2] S. Wang and G. Wallis, Phys. Rev. **105**, 1459 (1957).
[3] S. Wang and G. Wallis, Phys. Rev. **107**, 947 (1957).
[4] C. G. B. Garrett, Phys. Rev. **107**, 478 (1957).
[5] J. T. Law, Proc. Inst. Radio Engrs. **42**, 1367 (1954).
[6] J. T. Law and P. S. Meigs, J. Appl. Phys. **26**, 1265 (1955).
[7] E. N. Clarke, Phys. Rev. **99**, 1899 (1955).
[8] Eriksen, Statz, and deMars, J. Appl. Phys. **28**, 133 (1957).
[9] W. L. Brown, Phys. Rev. **91**, 518 (1953).

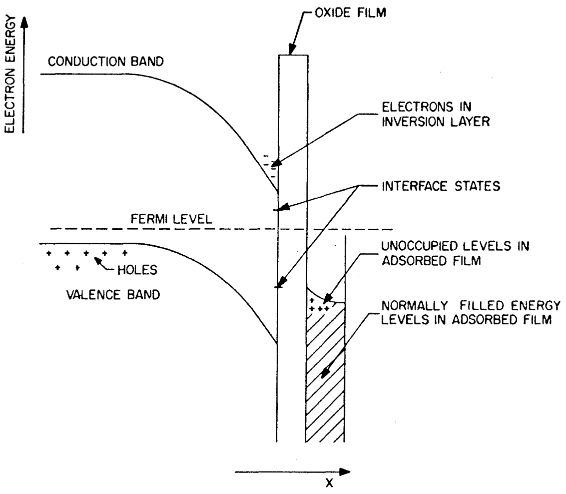

FIG. 1. Diagram of energy band near semiconductor surface with thick adsorbed film.

of the study of transient phenomena. For simplicity almost all measurements were carried out on *n-p-n* type grown silicon bars in ambients containing acetone vapor. Similar effects can be observed with water vapor and many other vapors and also with germanium samples.

ENERGY BAND DIAGRAM AT SURFACE

It has been shown by Law[5] that water vapor is adsorbed in a relatively thick layer on the surface. Germanium surfaces in ambients approaching 100% relative humidity may be covered with as many as ten monolayers of water molecules. It is believed that a similar situation exists for the adsorption of other vapors of certain organic liquids mentioned in reference 8. Gases like oxygen are adsorbed to a much smaller degree.[10] It is difficult to give an exact figure for the number of monolayers because most of the adsorbed oxygen is used for the formation of an oxide film. It appears likely, however, that the amount of adsorbed oxygen does not exceed one monolayer.

The liquids which will be discussed here give a positive surface charge. The energy bands on a *p*-type semiconductor with a thick adsorbed film are shown in Fig. 1. It is assumed that the highest occupied level in the liquid lies near the Fermi level. There thus exists a finite chance that some of the highest normally occupied levels are empty and a net positive charge resides in the adsorbed film. Since there are many liquid molecules packed close together, the molecules interact with each other and the sharp energy levels of the isolated molecules are split up in bands. If there is no periodicity in the adsorbed film, conventional energy band theory cannot be applied to calculate the density of states as a function of energy and calculations of the type developed by James and Ginzbarg[11] and by Parmenter[12–14] will have to be applied. Nevertheless, for the present purposes such calculations do not have to be carried out. Complicating features which arise from a different interaction of the first adsorbed monolayer with the oxide film will not be taken into account. It is clear from the experimental results that there is a positive charge in the adsorbed layers corresponding to from 10^{10} to more than 10^{12} charged molecules per cm^2, and thus the highest occupied band must lie within a few tenths of an electron volt of the Fermi level at the surface.

Consider now the effect of an electric field parallel to the surface. There appear to be two possible conduction mechanisms in the film. The first possibility is a hole conduction similar to the conduction-by-holes-mechanism in a semiconductor; that is, the individual molecules in the film remain fixed and the charge deficit jumps from molecule to molecule. The second mechanism is a quasi-ionic conduction in which the charged molecules, themselves, move until they lose their charge through the oxide film by a relaxation mechanism. Further below we shall show that the observed mobilities are relatively low; in particular, they have not been found to exceed substantially 10^{-3} $\text{cm}^2/\text{volt sec}$. In addition, the observed mobility is a strong function of the vapor pressure of the condensed liquid in the surrounding ambient. In ambients with lower vapor pressures the mobility may be smaller by orders of magnitude than that observed with a saturated ambient. One could attribute such a dependence to either conduction mechanism. It appears, however, that one should be able to distinguish between these two possibilities by an experiment carried out at sufficiently low temperatures so that the adsorbed liquid film is "frozen." All the evidence that has been collected in this laboratory indicates that the phenomena to be described below are still observable at temperatures far below the freezing point of the liquid in question, suggesting a mechanism of true hole conduction.

DISTRIBUTION OF CHARGE ALONG THE SURFACE

In this laboratory the study of the mobility of the outer surface charge started after the discovery of certain discrepancies between measurements of inversion layer conductance as a function of bias voltage in dry ambients[1,15] and in ambients containing vapors of water, methyl alcohol, pyridine, dioxane, acetone, and other liquids. In Fig. 2, a steady-state inversion layer conductance curve measured in the presence of acetone vapor is shown, as well as the circuit used for the measurements. All measurements were carried out

---

[10] *Semiconductor Surface Physics* (University of Pennsylvania Press, Philadelphia, 1957). See chapters by Green, Kafalas, and Robinson, p. 349; S. P. Wolsky and A. B. Fowler, p. 401.

[11] H. M. James and A. S. Ginzbarg, J. Phys. Chem. **57**, 840 (1953).

[12] R. H. Parmenter, Phys. Rev. **97**, 587 (1955).

[13] R. H. Parmenter, Phys. Rev. **99**, 1759 (1955).

[14] R. H. Parmenter, Phys. Rev. **99**, 1767 (1955).

[15] Statz, deMars, Davis, and Adams, Phys. Rev. **101**, 1272 (1956).

on *n-p-n* type grown silicon bars with a resistivity of the *p*-type region of 10 ohm cm. The width of the *p*-type region was 0.04 cm. The set-up was essentially identical to the one described in references 1 and 15. The sample preparation was also standard. Samples were etched in CP4, washed carefully in water, methyl alcohol and carbon tetrachloride and dried. They were then exposed to an ambient consisting of acetone vapor and nitrogen. Originally, it was believed[8] that the increasing conductance is due to a conductance in the adsorbed film superimposed on the inversion layer conductance. As will be shown in this paper, the processes giving this apparent increase in the conductance are quite involved but result from the finite mobility of the surface charge.

Let us first investigate the nature of the surface charge distribution on the inversion layer across the base region of an *n-p-n* type bar (Fig. 3). Consider the case in which the two *n*-regions are connected together and biased in reverse with respect to the *p*-region. Assume for the moment that the surface charge is immobile. The saturation current across the inversion layer bulk junction flows along the inversion layer to the *n*-sides and causes a parabolic potential profile [Fig. 3(b)]. If the surface charge is allowed now to move, it will flow from the ends towards the middle of the inversion layer [Fig. 3(c)]. The surface charge, however, is now out of equilibrium with the underlying bulk material and positive charge flows from the bulk into the surface film at the edges of the inversion layer and positive charge will flow into the bulk near the center of the base region. This charge relaxation has received attention in the literature.[16–18] It is well known that the rate of charge transfer is very sensitive to the thickness of the oxide film. A certain steady state charge distribution will be established on the surface.

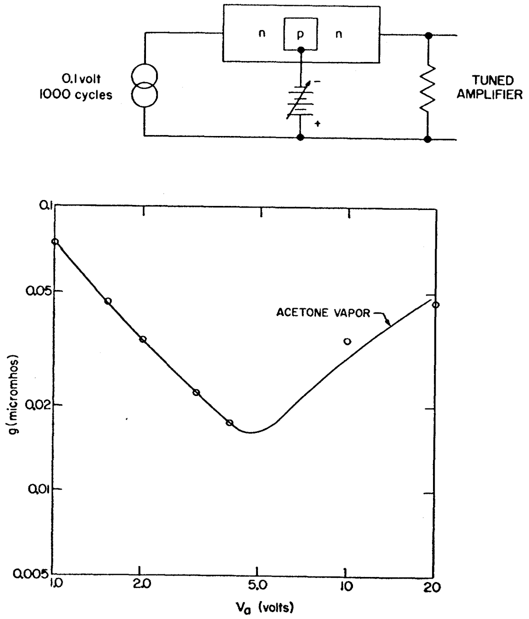

FIG. 2. Measuring circuit and curve of inversion layer conductance as a function of bias voltage.

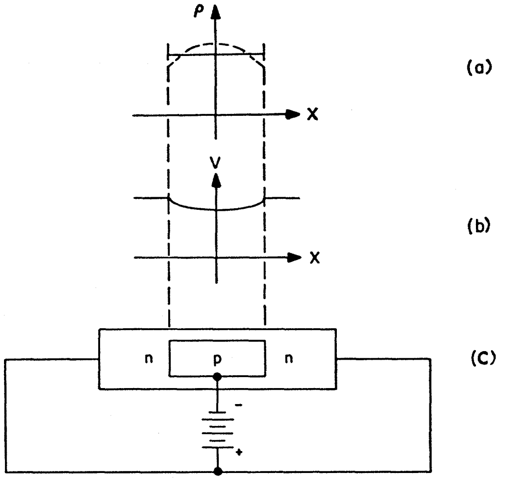

FIG. 3. Distribution of potential and surface charge density on reverse-biased inversion layer.

Let ρ be the positive charge density per unit area of surface. Its equilibrium density when the charge is immobile will be called ρ_0. This equilibrium value is known to be a function of the bias voltage. Its value increases with bias voltage.[1,15] The rate of flow of charge from the bulk through the oxide film into the adsorbed layer is given by $-(\rho-\rho_0)/\tau$, where τ is the phenomenological relaxation time of the outer surface states. We shall make the simplifying assumption that there is just one τ and not a spectrum of relaxation times. There is, however, evidence that in the ambients considered below a spectrum of relaxation times would give a better approximation. If $\mathbf{j}$ is the current density on the surface (current per unit length), the time derivative $\partial\rho/\partial t$ becomes

$$\partial\rho/\partial t=-(\rho-\rho_0)/\tau-\nabla\cdot\mathbf{j}. \tag{1}$$

If $\mathbf{E}$ is the component of the electric field in the surface, then

$$\mathbf{j}=\mu\rho\mathbf{E}-D\nabla\rho. \tag{2}$$

In Eq. (2), μ is the mobility and D is the diffusion constant of the surface charge. By inserting Eq. (2) into Eq. (1), one obtains

$$\partial\rho/\partial t=-(\rho-\rho_0)/\tau-\mu(\nabla\cdot\rho)\mathbf{E}-\mu\rho\nabla\cdot\mathbf{E}+D\nabla^2\rho. \tag{3}$$

For simplicity it will be assumed now that the potential along the surface is parabolic:

$$v=cx^2;\quad E_x=-\partial v/\partial x=-2cx. \tag{4}$$

---

[16] R. H. Kingston and A. L. McWhorter, Phys. Rev. **103**, 534 (1956).

[17] S. R. Morrison, Phys. Rev. **102**, 1297 (1956).

[18] Lasser, Wysocki, and Bernstein, Phys. Rev. **105**, 491 (1957).

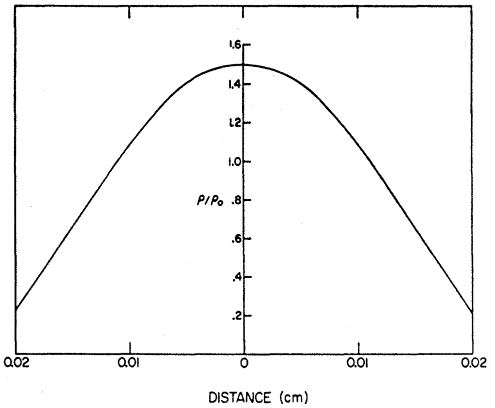

FIG. 4. Distribution of surface charge for a total voltage drop of 0.1 volt and a surface charge mobility of 10^{-3} cm²/volt sec.

This assumption would be correct if the conductance of the inversion layer were constant and much greater than that of the liquid film. Further below the modification of the inversion layer conductance is considered. The positive surface charge is neutralized by the electrons and the negative space charge in the semiconductor and no repulsion of the positive charges on the semiconductor surface has to be taken into account. Inserting Eq. (4) into Eq. (3) gives

$$\partial\rho/\partial t = -(\rho-\rho_0)/\tau + 2\mu c x\partial\rho/\partial x + c\mu\rho + D\partial^2\rho/\partial x^2. \quad (5)$$

Because of the symmetry of the problem, $\partial\rho/\partial x=0$ at $x=0$. We assume further $j(\pm x_0)=0$, where $\pm x_0$ represents the extension of the inversion layer. The latter condition is a simplification. The approximation is, however, under most circumstances good; on the n-type region there is very probably not much positive surface charge. Furthermore, holes in the adsorbed layer on the field-free n region can only get into the region of the inversion layer by the mechanism of diffusion. By introducing the dimensionless units: $R=\rho/\rho_0$; $T=t/\tau$; $L=x/(D\tau)^{\frac{1}{2}}$; $C=2c(q/kT)D\tau$; $V=v(q/kT)$ and by making use of the Einstein relation between μ and D, one obtains

$$\partial R/\partial T = 1+(C-1)R + CL\partial R/\partial L + \partial^2 R/\partial L^2. \quad (6)$$

In the reduced units the boundary conditions become

$$\begin{aligned} dR/dL &= 0 \qquad \text{for} \quad L=0, \\ d(\ln R)/dL &= \mp CL_0 \quad \text{for} \quad \pm L_0, \end{aligned} \quad (7)$$

where $L_0=x_0/(D\tau)^{\frac{1}{2}}$. First consider steady-state solutions for which $\partial R/\partial T=0$. The equation has to be integrated numerically. In order to reduce the number of parameters, we choose a value of x_0 equal to 0.02 cm, which agrees closely with the dimension of the experimental units, and a value of $\tau=1$ sec. As parameters, we consider the mobility μ of the holes in the liquid film and the total voltage drop v. The solutions to the equation were obtained on an analog computer. In Fig. 4, a typical solution is shown in which a potential drop of 0.1 volt and a mobility of 10^{-3} cm²/volt sec had been assumed.

In Table I, R at $L=0$ and $L=L_0$ is given for a series of values of μ and v. For mobilities greater than those given in Table I, the charge density is given very closely by a Boltzmann distribution. Even for relatively low mobilities the surface charge is nonuniformly distributed.

In the present model the outer surface states will not give a substantial contribution to inversion layer conductance, even if the high charge mobilities are assumed which had to be postulated previously.[8] The surface charge density becomes exceedingly low near the edges of the inversion layer and very little surface current could be carried in that surface region. These conclusions rest on the assumption of a relaxation time

TABLE I. Charge densities at center and edge of inversion layer for various mobilities and voltage drops.

Potential drop (volts)	Mobility $\left(\frac{\text{cm}^2}{\text{volt-sec}}\right)$ 10^{-5}	10^{-4}	10^{-3}	10^{-2}
0.002				$R_0=1.02$ $RL_0=0.96$
0.004				$R_0=1.09$ $RL_0=0.91$
0.01			$R_0=1.04$ $RL_0=0.86$	
0.02			$R_0=1.09$ $RL_0=0.74$	
0.04			$R_0=1.18$ $RL_0=0.54$	$R_0=1.45$ $RL_0=0.36$
0.06				$R_0=1.71$ $RL_0=0.21$
0.1			$R_0=1.50$ $RL_0=0.22$	$R_0=2.20$ $RL_0=0.07$
0.3		$R_0=1.18$ $RL_0=0.77$		
0.4				$R_0=5.64$ $RL_0=0.002$
0.5		$R_0=1.33$ $RL_0=0.031$		
0.8			$R_0=4.93$ $RL_0=0.004$	
1.0		$R_0=1.86$ $RL_0=0.002$		$R_0=17.0$ $RL_0=0.0002$
4.0			$R_0=17.0$ $RL_0=0.0002$	
8.0	$R_0=1.66$ $RL_0=0.003$	$R_0=12.0$ $RL_0=0.001$		
10.0		$R_0=15.4$ $RL_0=0.0005$		
40.0	$R_0=17.8$ $RL_0<10^{-4}$			

which is of the order of 1 sec. This assumption might be unjustified because the pileup of charge near the center of the inversion layer could cause some sort of breakdown in the oxide film due to the resulting high electric fields. This would reduce τ in the center considerably. Near the edges of the inversion layer, however, where the charge has moved away, the electric field across the oxide film is reduced and τ is expected to remain constant or possibly increase. It can be shown that a reduction of τ in the center would lead to a decrease in the surface charge density all over the surface of the inversion layer. Thus there still remains an almost nonconducting region near the edges of the inversion layer. This difficulty in the explanation of the surface conductance increasing with bias voltage gave rise to a more thorough investigation of the problem.

TRANSIENT BEHAVIOR OF INVERSION LAYER CONDUCTANCE

To check the original postulate that the charge in the outer surface states can move, the transient behavior of inversion layer conductance after switching of the bias voltage was investigated. Since the conductance of the inversion layer depends upon the charge in the surface states, one would expect to see variations in the conductance due to charge rearrangements in the outer surface states. In the experiments, inversion layer conductance was measured at a low bias voltage, for example, 2 volts. Then a short voltage pulse of up to 140 volts was applied. The pulse lengths varied from 10^{-5} to 1 sec; the voltage was chosen large enough to pinch off the inversion layer, at least in the beginning of the pulse. After the pulse, the variation of the conductance was recorded with a pen recorder or observed on an oscilloscope. There was a continuous transition in the observed curve shapes as the partial vapor pressure of the liquid (here acetone) was increased. The traces *a*, *b*, and *c* in Fig. 5 correspond to low vapor pressures. There are no noticeable effects due to the movement of charge in the adsorbed film. At the high voltage the charge in the outer surface states builds up with the characteristic time constant τ. By reducing the voltage again to the original value, the conductance is higher after the application of the voltage pulse and the charge decays again to its equilibrium value with the time constant τ. As the vapor pressure of the liquid was increased, a deformation of these curve shapes was observed. The traces *d* through *f* and *g* through *i* represent two typical sets of curves into which the traces *a* through *c* may deform with increasing acetone content. When the acetone vapor pressure was very high, the inversion layers, in general, were unstable, their conductance decreasing rapidly when any voltage was applied. One could still observe a transient conductance, however, by switching for a short time from a low voltage to an intermediate voltage and back again. The conductance would rise for some time to a finite value and then decay again to zero. The following section will investigate how the movement of charge in the outer surface states can explain the observed curve shapes.

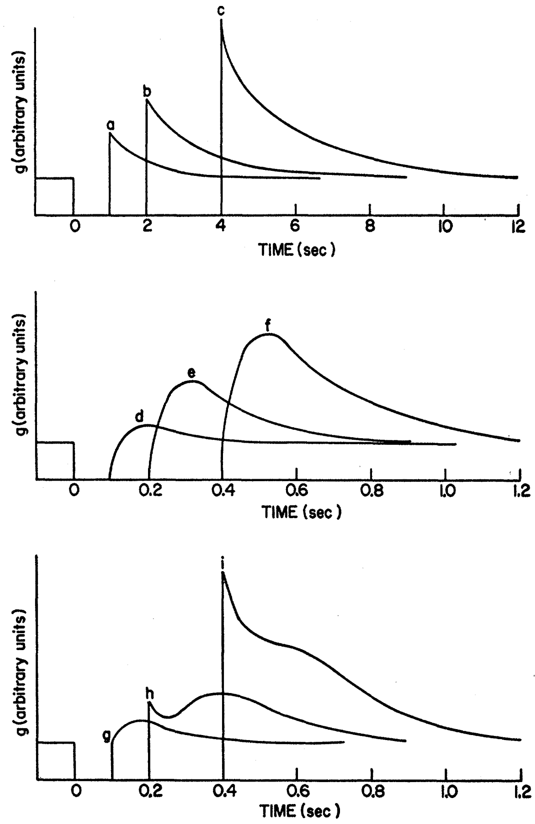

FIG. 5. Inversion layer conductance transients after application of a bias voltage pulse.

SIMPLIFIED ANALYSIS OF TRANSIENTS

Several simplifications will be made in this analysis. Not all of the charge inducing the inversion layer is mobile; there will be some charge in interface states. This latter charge will be neglected. We shall consider the problem first without taking into account the variation in the conductance of the underlying inversion layer due to changes in the charge density on the surface. There is no easy way to include in the calculations the phenomenon of pinch-off. We shall approximate pinch-off first by an inversion layer with a low conductance; i.e., the inversion layer will be considered to produce a relatively large voltage drop along the surface due to the saturation current. Further below we shall see how the results change if we do not make these assumptions.

The problem is described by a solution of Eq. (6) with the boundary conditions (7). To solve this equation we shall consider the values of R only at certain points: $L=0$, $\Delta l\cdots i\Delta l\cdots n\Delta l$. Because of the symmetry of the problem, only positive values of L have to be considered. These values of R will be denoted by R_0, $R_1\cdots R_n$. The differentials $\partial R/\partial L$ and $\partial^2 R/\partial L^2$ will be replaced by difference expressions. Equation (6) with Eq. (7) gives

$$\begin{aligned} \frac{\partial R_i}{\partial T} &= 1+(C-1)R_i+iC\frac{R_{i+1}-R_{i-1}}{2} \\ &\quad +\frac{R_{i+1}-2R_i+R_{i-1}}{\Delta l^2} \quad \text{for} \quad 1\leqslant i\leqslant n-1, \\ \text{and} \qquad \frac{\partial R_0}{\partial T} &= 1+(C-1)R_0+2\frac{R_1-R_0}{\Delta l^2}, \\ R_n &= \frac{1}{\frac{3}{2}+\Delta l C L_0}(2R_{n-1}-\tfrac{1}{2}R_{n-2}). \end{aligned} \tag{8}$$

This simultaneous set of differential equations for $R_i(T)$ can be readily solved on an analog computer. In the present case, twelve intervals were chosen. For simplicity, at the low voltage no voltage drop will be assumed. The equilibrium charge density at this voltage will be designated by ρ_L. In switching to the high voltage the inversion layer conductance decreases and a voltage drop due to the saturation current will be assumed. The equilibrium charge density in the absence of any voltage drop will be called ρ_H. ρ_H has a larger value than ρ_L. For a more detailed description as to how the equilibrium charge increases with applied voltage, the reader is referred to references 1 and 15. In the experiments this ratio ρ_H/ρ_L was approximately 1.25.

In Fig. 6(a), a specific example is shown. The mobility of the holes in the liquid film is assumed to be 10^{-3} cm^2/volt sec, the relaxation time τ is taken to be 1 sec, the voltage drop along the inversion layer is taken to be 0.04 volt. These numbers give $L_0=4$ and $C=0.2$. Figure 6(a) shows how the distribution of charge changes on the surface as a function of time when the high voltage is applied. We consider now what happens when the pulse is terminated; i.e., C will be set to zero when the charge distribution has reached the shape which is indicated by a dashed line. Figure 6(b) shows how the charge relaxes back again into its original shape. Before discussing the effects of this redistribution, consider qualitatively the changes in Fig. 6 if a different mobility of the charge in the surface film is assumed. If the mobility is much higher, the charge redistributes itself faster and the slow relaxation through the oxide film does not disturb the distribution too much. For example, if we allow the dashed distribution of Fig. 6(b) to relax back to its equilibrium value with a much higher mobility, the charge first spreads out very fast to a constant value from $-L_0$ to $+L_0$. The area under this curve is practically identical to that under the dashed curve. Then the distribution relaxes slowly back to its equilibrium value, with the characteristic time constant τ, always retaining the rectangular shape. In other words, the time $t(\approx x_0^2/D)$ for the charge to spread out over the surface of the sample is short as compared to the relaxation time τ. If, on the other hand, a very small mobility is used, the movement of the charge can be neglected and the charge relaxes back at each point to its constant equilibrium value with the characteristic time constant τ.

To see from this simplified model how the conductance of the inversion layer varies with time, we shall first investigate the dependence of that conductance on the surface charge. The energy bands of a p-type sample with a positive charge on the surface are shown in Fig. 7. The number of electrons n per unit square of

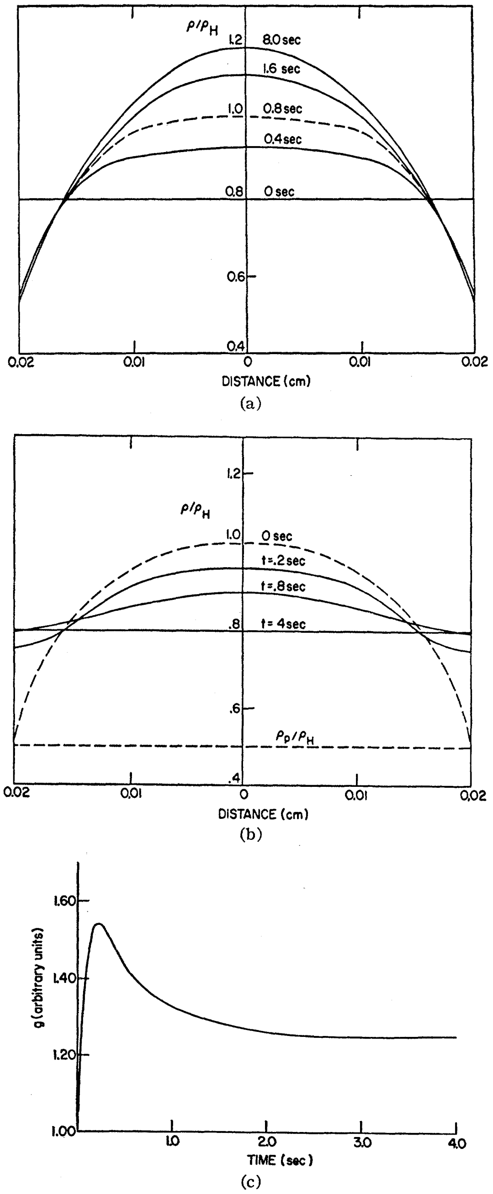

FIG. 6. (a) Change in surface charge distribution with time after the application of a bias voltage. (b) Relaxation of surface charge distribution to its original shape after removal of bias voltage. (c) Inversion layer conductance after removal of the bias voltage, as deduced from 6(b).

inversion layer skin is given by[15]

$$n\approx\left(\frac{\epsilon}{2\pi}\right)^{\frac{1}{2}}\left(\frac{1}{q}\right)\left\{\rho_a\left(|V_a|+|\Psi_p|+|\phi_s|-\frac{kT}{q}\right)+\frac{kT}{q}qn_i\exp\left(\frac{q}{kT}|\phi_s|\right)\right\}^{\frac{1}{2}}-\left(\frac{\epsilon}{2\pi}\right)^{\frac{1}{2}}\left(\frac{1}{q}\right)\times\left\{\rho_a\left(|V_a|+|\Psi_p|+|\phi_s|-\frac{kT}{q}\right)+\frac{kT}{q}qn_i\right\}^{\frac{1}{2}}. \quad (9)$$

Equation (9) corresponds to Eq. (13) of reference 15. (The subscripts d have been replaced by a since we are dealing here with a p-type sample.) ϵ is the dielectric constant, q is the electronic charge, ρ_a is the charge density due to the ionized acceptors, k is Boltzmann's constant, T is the absolute temperature, and n_i is the intrinsic density of electrons. The meaning of the other symbols may be obtained from Fig. 7. Similarly, it has been shown in reference 15 that the surface charge ρ_s per unit square of skin is given by

$$\rho_s=\left(\frac{\epsilon}{2\pi}\right)^{\frac{1}{2}}\left\{\rho_a\left(|V_a|+|\Psi_p|+|\phi_s|-\frac{kT}{q}\right)+\frac{kT}{q}qn_i\exp\left(\frac{q}{kT}|\phi_s|\right)\right\}^{\frac{1}{2}}. \quad (10)$$

Thus, one can write:

$$n=(1/q)(\rho_s-\rho_p), \quad (11)$$

where

$$\rho_p=\left(\frac{\epsilon}{2\pi}\right)^{\frac{1}{2}}\left\{\rho_a\left(|V_a|+|\Psi_p|+|\phi_s|-\frac{kT}{q}\right)+\frac{kT}{q}qn_i\right\}^{\frac{1}{2}}. \quad (12)$$

Since ϕ_s is always a very small quantity in comparison with the applied voltage, ρ_p may be considered to be a constant. ρ_p stands for $\rho_{\text{pinch-off}}$ because $n=0$ for $\rho_s=\rho_p$. The conductivity g of the inversion layer is given by $g=q\mu_e n$, where μ_e is the mobility of the electrons in the inversion layer. μ_e can be considered a constant independent of ρ_s as long as the electronic charge does not become comparable to the negative charge due to the ionized acceptors, i.e., for all inversion layers except the strongest ones. If one uses Fig. 6 to compute the inversion layer conductance, it does not matter much what value of ρ_p is assumed, since the same shape of curve is obtained. In Fig. 6(b), the value of ρ_p used in the calculations is indicated by a horizontal dashed line. The inversion layer conductance corresponding to a given curve in Fig. 6(b) is given by the following:

$$\frac{1}{g}=\text{constant}\left[\frac{1}{2}\left(\frac{1}{\rho_0-\rho_p}+\frac{1}{\rho_{12}-\rho_p}\right)+\sum_{i=1}^{11}\frac{1}{\rho_i-\rho_p}\right], \quad (13)$$

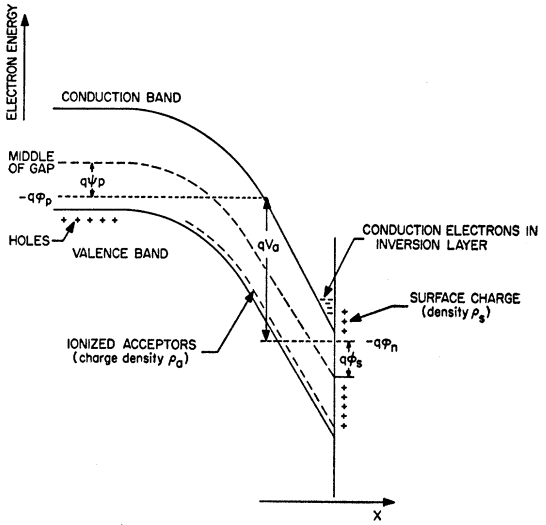

FIG. 7. Energy bands near surface on a p-type semiconductor with a net positive surface charge.

where the indices $0\ldots i\ldots 12$ refer to the stations on the analog computer.

g is plotted in arbitrary units in Fig. 6(c) as a function of time. The result may be stated: When a large potential drop exists along the surface, charge will flow from the edges to the center of the inversion layer. Thus, the edges of the inversion layer are conducting poorly. When the potential drop is suddenly reduced, the resulting flow of charge to the ends of the inversion layer makes itself felt first by increasing the over-all conductance of the inversion layer. Then, the charge approaches its new lower equilibrium value, corresponding to the lower applied voltage, and the conductance of the inversion layer decreases to its equilibrium value. Figure 6(c) resembles the experimental curves 5d through 5f. For charge mobilities in the adsorbed film of the order of 10^{-2} cm^2/volt sec and lower, the direct contribution of the film conductance to the inversion layer conductance is entirely negligible.

We shall now investigate the influence of a more adequate treatment of the pinch-off phenomenon on the results. As a first step, we want to consider the potential distribution along the surface when a voltage larger than the pinch-off voltage is applied. For a definition of the coordinate axes, see Fig. 8. Let the positive surface charge be ρ_s. At the pinch-off voltage there will be no free carriers left and the energy bands will be bent approximately by an amount $\bar{V}$,

$$\bar{V}=(2\pi/\epsilon)(\rho_s^2/\rho_a), \quad (14)$$

the potential as a function of y being given by

$$\bar{V}=(2\pi/\epsilon)\rho_a y^2. \quad (15)$$

The surface is located at $y_{\max}=\rho_s/\rho_a$. If the applied voltage is raised by an amount $\Delta\bar{V}$ above pinch-off, the potential will no longer be independent of x. An analytic

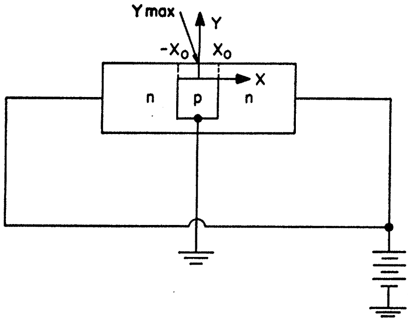

FIG. 8. Choice of coordinate axes for calculation of potential distribution under pinch-off conditions.

solution in closed form, however, can only be given if we modify the problem somewhat. Suppose that for $y<0$, the semiconductor is so heavily doped that the space-charge layer cannot penetrate any further into the p-type material. As may be checked easily, the following solution then satisfies Poisson's equation:

$$\bar{V}=\frac{2\pi}{\epsilon}\rho_a y^2+\frac{\Delta\bar{V}}{\cosh\left(\dfrac{\pi}{2}\dfrac{x_0}{y_{\max}}\right)}\cosh\left(\frac{\pi}{2}\frac{x}{y_{\max}}\right)\times\sin\left(\frac{\pi}{2}\frac{y}{y_{\max}}\right). \quad (16)$$

Equation (16) also satisfies the boundary conditions $(d\bar{V}/dy)_{y_{\max}}=(4\pi/\epsilon)\rho_s$ and $\bar{V}=0$ for $y=0$. It is interesting to note that the additional voltage $\Delta\bar{V}$ drops within a few $y_{\max}$ of the edges of the inversion layer. The potential on the surface of the inversion layer, with the exception of the short edges, equals the pinch-off voltage. Equation (16) does not take into account complications which arise from the finite width of the space-charge regions of the main p-n junctions.

Thus, at voltages beyond pinch-off, strong fields existing at the edges of the inversion layer tend to move all the positive surface charge towards the field-free middle region of the inversion layer. Unfortunately, Eq. (16) does not give these field strengths accurately because of the above-mentioned simplifications. One may estimate, however, that these field strengths are of the order of 10^4 volts/cm, and a very rapid removal of the mobile surface charge is expected. In the previous calculations it has been assumed that the potential distribution is parabolic, thus underestimating the high fields at the edges. However, the explanation of curves 5d through 5f remains essentially the same. While the inversion layer is pinched off, all the surface charge flows away from the edges of the inversion layer. When the pulse is removed, the inversion layer in the vicinity of x_0 is nonconducting. As the charge of the middle part of the inversion layer spreads, the conductance of these edge regions rises and the measured over-all conductance increases. The conductance at the maximum is related to the amount of charge that has been created during the high voltage pulse; thus, one expects that the maximum conductance increases with the pulse duration.

The traces of Fig. 5, g through i, may be explained with the help of the following section. It will be shown there that, at a certain bias voltage, an inversion layer with a mobile charge may be stable or unstable, depending upon the relative magnitude of certain parameters. In Fig. 5(g), the inversion layer is essentially pinched off after the removal of the pulse. However, if the pulse is applied long enough, sufficient charge may move through the oxide film for the inversion ayer to be stable. There will still be a slight depletion of charge near the edges of the inversion layer, but not sufficient to pinch off the inversion layer. The spreading of the charge gives the slight bump in the decaying conductance curve i of Fig. 5. Curve h of Fig. 5 lies in between the curves g and i. There is evidence that quite frequently nonuniformities account for these curves. A part of the channel may be essentially stable and give rise to a conductance of the type shown in the traces a to c and other parts of the inversion layer may

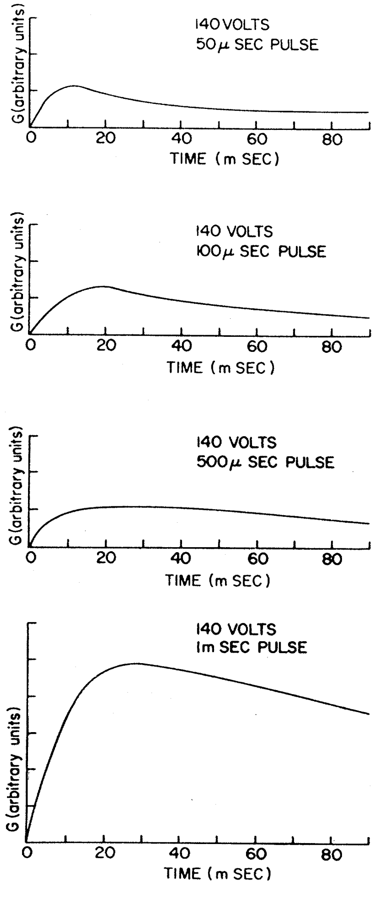

FIG. 9. Measured inversion layer conductance after the application of bias voltage pulses of various durations.

give a conductance behavior as presented in Fig. 5, curves d to f. The superposition of the two will then give curves as shown in Fig. 5, curves g to i.

One may use curves of the type shown in Fig. 5, curves d through f, to estimate the mobility of the surface charge. A sample was held in an atmosphere almost saturated with acetone vapor. The response was expected to be fast due to the relatively thick adsorbed film with its resultant high mobility of surface charge. Pulses of 140 volts with durations varying from 5×10^{-5} sec to 10^{-3} sec were applied. The resulting conductance curves plotted as a function of time are shown in Fig. 9. In order to obtain a complete pinch-off, it is estimated that the surface charge has to be removed over a distance of about twice the thickness of the inversion layer, i.e., about 3×10^{-4} cm near the main junctions. Assume further an average electric field in that region of 10^4 volts/cm. In order for this charge removal to take approximately 5×10^{-5} sec (Fig. 9), the mobility of the charge must be about 6×10^{-4} cm^2/volt sec. From the recovery of the conductance, one may obtain another estimate of the mobility. Assume again that the charge was reduced over a region of $d=3\times10^{-4}$ cm, the time for the charge on the middle portion of the inversion layer to spread out will be approximately $t=(d^2/D)=(q/kT)(d^2/\mu)$. Since t is about 8×10^{-3} sec, one obtains $\mu=5\times10^{-4}$ cm^2/volt sec. The latter value tends to overestimate the mobility somewhat since the charge generation through the oxide film by the relaxation mechanism has been neglected. However, the two methods of determining μ agree satisfactorily indicating that our model is essentially correct. Better and more convenient methods for measuring the mobility of the surface charge are presently being worked out. It appears that in thick films of adsorbed acetone vapor the charge mobility is of the order of 10^{-3} cm^2/volt sec, but in thin films the mobility may be many orders of magnitude smaller.

It may be mentioned at this point that there appears to be some correlation between the surface charge mobility and the spectrum of relaxation times. In general, it is observed that for higher surface charge mobilities the relaxation times become shorter. The reason for this correlation has not yet been investigated.

STABILITY OF INVERSION LAYERS IN THE PRESENCE OF MOBILE CHARGES IN THE ADSORBED FILM

In the previous calculations relating to Fig. 3, the dependence of the conductivity of the inversion layer on the surface charge was not considered. Considering now this dependence, one can easily visualize, with the help of Fig. 3, that inversion layers may be unstable. In Fig. 3(c), the charge as a function of x is shown by a dashed line. For the calculation of this charge density, a parabolic potential was assumed. The reduction of the charge density at the edges of the inversion layer, however, decreases the conductivity in the underlying inversion layer, and the potential rise is faster than parabolic. This new potential, in turn, makes more surface charge move towards the center and the conductivity of the inversion layer at the edges becomes still smaller. This process may continue until the inversion layer pinches off.

To obtain more quantitative insight into this stability problem, consider first the case where the movement of the charge in the adsorbed film is so fast that the charge transfer mechanism through the oxide film can be neglected. This means, for example, that the term $(\rho-\rho_0)/\tau$ in Eq. (3) can be neglected. We shall further consider a steady-state problem, $\partial\rho/\partial t=0$. Solving Eq. (3) then gives

$$\rho=\rho_d\exp(-qV/kT), \tag{17}$$

where ρ_d is some constant. The conductance of the inversion layer is given by

$$g=\mu_e(\rho-\rho_p). \tag{18}$$

In Eq. (18), μ_e is the mobility of an electron in the inversion layer. Equation (18) is only valid as long as $\rho>\rho_p$. Furthermore,

$$\frac{dV}{dx}=\frac{1}{g}I(x), \tag{19}$$

where $I(x)$ is the surface current density in the inversion layer. We may assume a constant saturation current j_0 across the surface junction and write:

$$I(x)=j_0x. \tag{20}$$

Equation (19) may now be integrated to give

$$\frac{kT}{q}\left(\frac{2\mu_e}{j_0}\right)\left\{\rho_d\left[1-\exp\left(-\frac{qV}{kT}\right)\right]-\frac{q}{kT}\rho_pV\right\}=x^2. \tag{21}$$

The inversion layer will pinch off at a point where

$$\rho_p=\rho_d\exp(-qV/kT). \tag{22}$$

By inserting Eq. (22) into Eq. (21), one obtains

$$x^2=\frac{2\mu_e}{j_0}\left(\frac{kT}{q}\right)\left\{\rho_d-\rho_p-\rho_p\ln\left(\frac{\rho_d}{\rho_p}\right)\right\}$$

$$\approx\frac{kT}{q}\left(\frac{\mu_e}{j_0}\right)\left[\frac{(\rho_d-\rho_p)^2}{\rho_p}\right]. \tag{23}$$

ρ_d is still an unknown number. From Eq. (1) and the boundary conditions, it follows that the average charge density $\bar{\rho}$, in the presence of fields, is equal to the equilibrium charge density ρ_0. For an estimate of typical values of x, it will be sufficient to assume ρ_d equals ρ_0. Assume: $\rho_0=(1.1\times10^{11})$ (1.6×10^{-19}) amp sec/cm^2; $\rho_p=(1.0\times10^{11})$ (1.6×10^{-19}) amp sec/cm^2; $\mu_e=10^3$ cm^2/volt sec; $j_0=10^{-5}$ amp/cm^2 and $kT/q=0.025$ volt. One

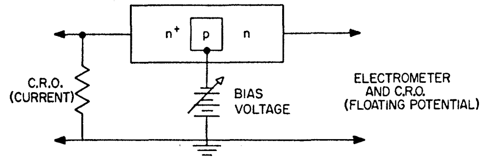

FIG. 10. Circuit for the measurement of floating potential and/or reverse current.

then obtains $x=2\times10^{-2}$ cm. Thus for the inversion layer not to pinch off, the *p* region of the *n-p-n* bars could be 4×10^{-2} cm wide. If one neglected the movement of the charge, the voltage drop due to the saturation current would be 1.25×10^{-3} volt for the above example, as compared with the actual voltage drop of 2.4×10^{-3} volt.

Let us next consider the physical significance of the case where the calculated value of x comes out smaller than the dimensions of the inversion layer. At the point where the inversion layer pinches off, a large voltage drop appears because the inversion layer becomes essentially nonconducting. Because of this drop, the bias voltage of the middle part of the inversion layer becomes substantially smaller. For a smaller bias voltage, one has new values of ρ_0 and ρ_p such that the value $(\rho_0-\rho_p)$ in Eq. (23) becomes larger. Thus a new, greater x^2 can be calculated. The inversion layer will assume such a voltage that the calculated pinch-off point is at the junction. This can be seen in various ways: Assume contrary to the above statement that the pinch-off points would lie symmetrically to the middle of the inversion layer some distance before the main *p-n* junctions. Since, at the pinch-off point, there will be a substantial voltage drop, the charge density ρ equal to $\rho_d \exp(-qV/kT)$ will have a very small value beyond the pinch-off point. Such a small charge density cannot, however, support an inversion layer and there would be no conducting channel through which the collected saturation current could flow into the *n* regions. If the voltage of the inversion layer becomes comparable to or smaller than kT/q, not all of the saturation current is collected. This case occurs quite frequently in our experiments. There are also additional complicating features present: Either the saturation current or the inversion layer conductance may be nonuniform, resulting in regions where all the saturation current is collected and others where it is not. With these reservations, let us next study the experimental verification of this charge rearrangement. For this purpose, a large voltage step is fed in between one *n*-type side and the *p*-type base of an *n-p-n* structure as shown in Fig. 10. The floating potential of the other *n*-type side, with respect to the base, is measured with an electrometer. This floating potential corresponds to the potential of the inversion layer at the extreme right with respect to the *p*-region. As the pulse is applied, the potential of the *n*-region rises to the pinch-off voltage, defined as that voltage at which, with constant surface charge density, no carriers are left in the inversion layer. Then, the charge slowly rearranges and the inversion layer assumes such a voltage that the previously defined pinch-off occurs just at the left-hand *p-n* junction. The floating potential as a function of time is shown in Fig. 11(a) for a case in which the ambient was almost saturated with acetone vapor. Another case is shown in Fig. 11(b). A voltage step of 80 volts is applied. The floating voltage immediately rises to 80 volts. Apparently the pinch-off voltage in this case is larger than 80 volts. Then the charge rearrangement takes place and the floating potential drops. However, at this

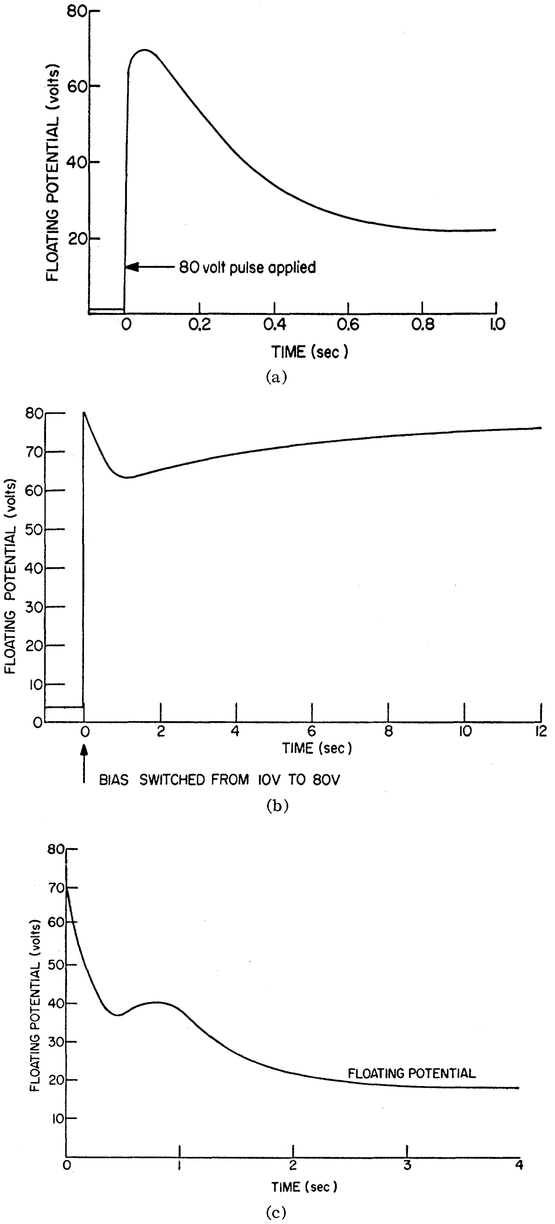

FIG. 11. Floating potential following an increase in bias voltage for various surface conditions.

higher voltage there is a larger equilibrium charge in the outer surface states. The charge builds up with the characteristic time constant of the outer surface states. With the increasing charge the floating potential rises again. In Fig. 11(a), the relaxation time was apparently much shorter than the time required for the charge redistribution. In Fig. 11(c), a case is shown in which the two time constants are approximately equal and the effect of the charge increase becomes apparent through a wiggle in the curve representing floating potential as a function of time. One can also perform the inverse experiment. With a high voltage applied for some time, there is a charge rearrangement such that there is a small region in the vicinity of the bulk junction with almost no mobile surface charge. When the applied voltage is reduced, this charge depleted region will be larger than it would be under equilibrium conditions at the low voltage. Thus, upon switching the voltage to the lower value, the floating potential goes to a lower than equilibrium value as is shown for a specific case in Fig. 12, where the voltage was switched from 180 volts to 10 volts. As the charge spreads out, the floating potential rises. The charge then decays to its low-voltage equilibrium value and the floating potential drops again. Similar curves are obtained for the reverse current, as shown in Fig. 13, where the voltage was switched from 170 volts to 0.5 volt. More experimental evidence for the existence of a charge depleted region will be presented in the next section.

From Figs. 11 and 12, it is apparent that it takes a finite time for the charge to redistribute and that the simplified calculation with very large values for μ and τ is not justified. More correctly, Eq. (3) with Eqs. (18), (19), and (20) gives

$$-\frac{\rho-\rho_0}{\tau}+D\frac{q}{kT}\frac{j_0}{\mu_e}\left[\frac{x(\partial\rho/\partial x)}{\rho-\rho_p}\right]+D\frac{q}{kT}\frac{j_0}{\mu_e}\left(\frac{\rho}{\rho-\rho_p}\right)$$
$$-D\frac{q}{kT}\frac{j_0}{\mu_e}\left[\frac{x\rho(\partial\rho/\partial x)}{(\rho-\rho_p)^2}\right]+D\frac{\partial^2\rho}{\partial x^2}=0. \qquad (24)$$

The boundary conditions are:

$$\partial\rho/\partial x=0 \qquad \text{for} \quad x=0;$$
$$\frac{\partial\rho}{\partial x}=\mp\frac{q}{kT}\frac{j_0}{\mu_e}\left(\frac{x\rho}{\rho-\rho_p}\right) \quad \text{at} \quad x=\pm x_0. \qquad (25)$$

The problem is to see whether there are solutions satisfying the boundary conditions with $\rho\geq\rho_p$ in the whole interval. In the region where no pinch-off was found with the previous method, Eq. (24) will also have a solution. If D is small enough, Eq. (24) can also have a solution in the region where the previous method indicated a pinch-off between $0<x<x_0$. This occurs because the charge near $x=\pm x_0$ is larger than calculated previously, due to the transport of charge from the bulk to the adsorbed film.

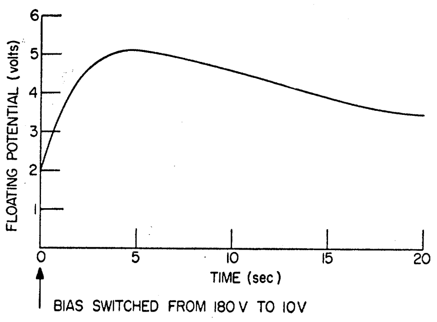

FIG. 12. Floating potential following a reduction in bias voltage.

No analytical solutions of Eq. (24) have been found. By numerical methods, however, solutions can be obtained. Consider an example. The width of the base region of the *n-p-n* bar is 0.04 cm in the samples employed for the described experiments. If expressed in units of the electronic charge, ρ_0 and $\rho_0-\rho_p$ are assumed to be 2×10^{11} and 3.45×10^9 charges/cm^2, respectively. With $\mu_e=500$ cm^2/volt sec, the latter value corresponds to an equilibrium inversion layer conductance of 0.276 μmho. If the charges could not move, a saturation current $j_0=10^{-4}$ amp/cm^2 would give a potential drop of 0.075 volt$\approx3kT/q$. If τ is assumed to be 1 sec, an approximate solution of Eq. (24) shows that, at some value of D between 10^{-9} and 10^{-10} cm^2/sec, the inversion layer would not pinch off due to the movement of charge.

For cases in which D becomes small, the boundary conditions become more critical. If there is a steep potential drop in the region where the inversion layer meets the main *p-n* junctions, the current in the liquid film can no longer be strictly zero at $x=\pm x_0$. The surface charge that is generated in this high-field region will flow into the inversion layer region. The high-field region will, in general, become larger as the potential drop between the inversion layer and the *n*-type sides increases. That an effect of this sort is important may be deduced from measurements of the type shown in Fig. 11. In general, it is found that the steady-state floating potential increases as the applied voltage is increased. If the boundary conditions would remain the same and independent of the applied voltage, the

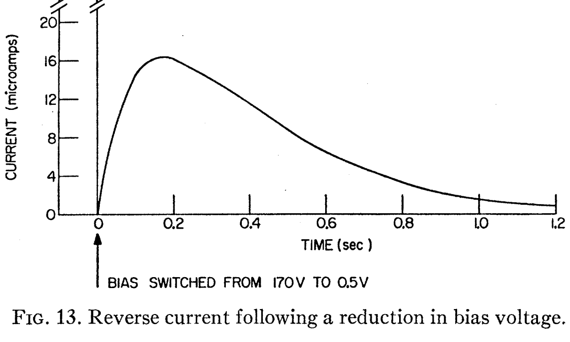

FIG. 13. Reverse current following a reduction in bias voltage.

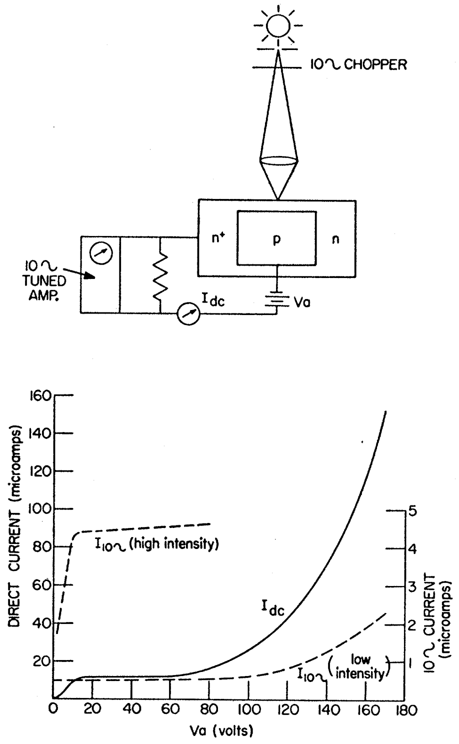

FIG. 14. Measuring circuit and curves of reverse current and photocurrent as a function of applied voltage.

floating potential of the inversion layer should also remain constant.

SURFACE CURRENT MULTIPLICATION

It has been shown that high electric fields may exist where the inversion layer meets the *p-n* junctions. From measurements of diode characteristics, it became apparent that surface current multiplication can take place in this high-field region at total applied voltages which are lower than those required for multiplication in the bulk junction. In Fig. 14, a steady-state diode characteristic is shown which was measured with the voltage applied between the n^+ side and the base region. Between zero and ten volts the current increased rapidly. Then a region was found in which the direct current is approximately independent of voltage. At higher voltages the direct current further increased with increasing voltage. The first increase in current between zero and ten volts is believed to result from the gradual increase in floating potential to values substantially above kT/q at all points. Above an applied voltage of ten volts all saturation current is collected. At the higher voltages the current increases due to current multiplication in the high field regions near the junction. To check these postulates, a ten cycles per second chopped light beam was focused on the surface and the resulting photocurrent was measured. The results, together with the experimental arrangement, are shown in Fig. 14. At low light intensities, and at low voltages, the photocurrent was approximately constant. At the higher voltages, where multiplication took place, the photocurrent increased; however, not as much as the direct current. In general, the multiplication was found to be nonuniform around the junction and the difference in the multiplication of the photocurrent and the direct current is attributed to these inhomogeneities. In dry ambients the multiplication factor of the bulk junction at 180 volts was close to one and not more than two. This surface current multiplication had also previously been found by Bernstein and Kingston[19] for germanium *n-p-n* bars in ambients containing water vapor. These authors find that multiplication sets in at relatively low voltages long before multiplication is observed in dry ambients. At that time (1955), of course, nothing was known about the movement of surface charge and its implications. Probably some of the experiments of Garrett and Brattain[20] are also related to the experiments described in this section. To check the postulate that the increase in current between zero and ten volts results from an increase in the floating potential to values substantially above kT/q, the light intensity of the chopped beam was increased by a factor of almost ten. This higher photocurrent now loads the inversion layer and produces a larger potential jump at the main junction in the region where the photocurrent enters the n^+ region. For the higher light intensity, a total voltage of 10 volts was required before all the photocurrent was collected. A similar measurement was made using the other *p-n* junction. Over the same voltage range no evidence of current multiplication was found.

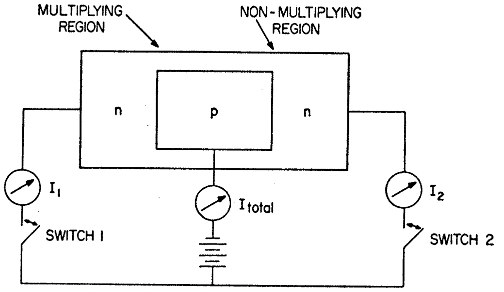

FIG. 15. Measuring circuit for determination of multiplying region.

In order to show conclusively that current multiplication takes place in the high-field region near the junction and not in the junction between the bulk and the inversion layer, the experiment shown in Fig. 15 was performed. With switches 1 and 2 closed, a high enough voltage was applied to cause surface current multiplication to occur at the left p-n^+ junction but not at the right *p-n* junction. The total current was meas-

---

[19] H. Bernstein and R. H. Kingston, Phys. Rev. **98**, 1566(A) (1955).

[20] C. G. Garrett and W. H. Brattain, J. Appl. Phys. **27**, 299 (1956).

ured in the base lead. When switch 1 was opened, the total current decreased. However, when switch 2 was opened, with switch 1 closed, the total current increased. This behavior of the current is readily explained. When switch 1 is open, current no longer flows through the multiplying region. All the surface saturation current now has to flow through the nonmultiplying region and there is a decrease in the total current as the multiplication mechanism is no longer operative. If the switch 2 is open, all the collected surface current flows through the multiplying region and there is an increase in the total current. At lower voltages, where there was no multiplication, only a slight decrease in total current was observed after opening either switch 1 or switch 2.

In Fig. 16, the time dependence of the direct current and the chopped photocurrent is shown when the voltage was switched from 2 to 175 volts. The voltage was applied between the n^+ side and the base region. The multiplication factor jumps to the rather high value of 35 as deduced from the photocurrent. The multiplication then decreases and, initially, the direct current follows the decrease of the multiplication. The direct current then rises substantially and finally decreases again slightly. The increase in the current is believed to result from an increase in the floating potential at all points to values substantially above kT/q such that at the current maximum all saturation current is collected. As the floating potential rises, the multiplication decreases. Apparently, for some time the increase in the collected current outweighs the decrease in the multiplication.

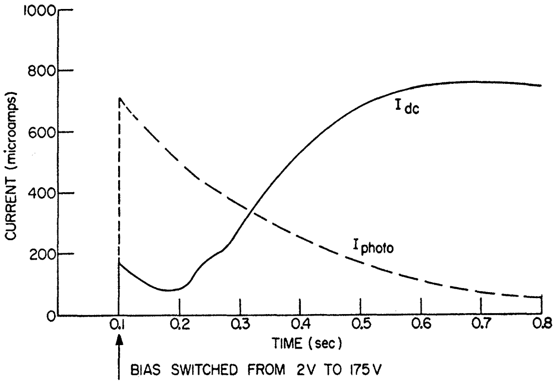

FIG. 16. Reverse current and photocurrent following an increase in bias voltage.

Finally, consider the mechanism for the current multiplication. It is difficult to estimate the field strength at the surface correctly. If there were no charge on the surface, the field would then, of course, be the same as in the bulk junction. In order to explain the surface current multiplication and surface breakdown at the lower applied voltages, one may either assume that the field strength on the surface is the same as in the bulk and look for a multiplication mechanism different from the regular avalanche mechanism, or one may consider conditions under which the surface field is larger than in the bulk. As an example for a mechanism giving a multiplication at a lower field strength, one might consider the impact ionization of interface states in the high-field region. Obviously, smaller field strengths are required to excite electrons from interface states to the conduction band, or electrons from the valence band to interface states, than to induce valence to conduction band transitions. A mechanism resulting in an increased field is shown in Fig. 17. Here, a negative surface charge is depicted as increasing the field at the surface to values larger than those found in the bulk junction. Such a negative surface charge might result if the interface states were to have a net negative charge. As explained above, the positive surface charge is mobile and has moved out of the high-field region.

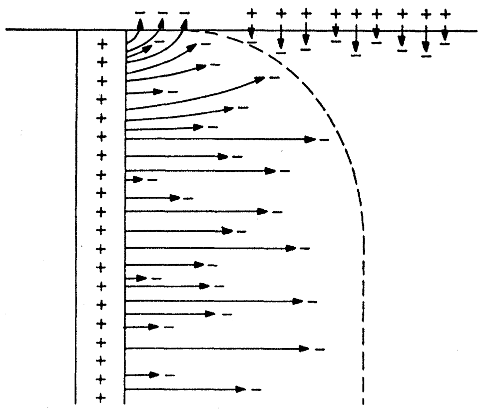

FIG. 17. Possible configuration of space charge near surface.

There are indications from measurements of the density of outer surface states per unit area and energy interval that simultaneously there are different types of outer surface states present. Suppose that there is a minority of negatively charged surface states, for example, of the type produced by oxygen. If this negative charge were immobile, and if enough positive charge would move away, the field configuration shown in Fig. 15 would also be produced.

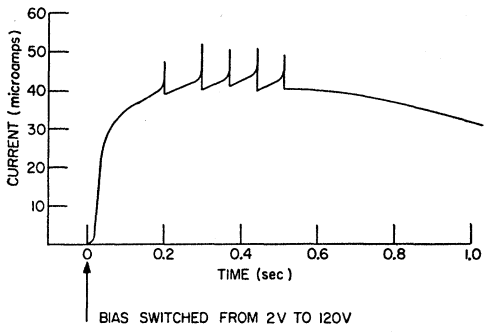

FIG. 18. Current spikes at onset of surface current multiplication.

Interesting in this connection is the observation of current spikes of about 10 μa in magnitude at the onset of surface current multiplication. A curve showing these spikes is given in Fig. 18. The voltage was switched from 2 to 120 volts. With an applied potential which is a few volts higher many more spikes are present. This observation indicates that the same microplasmas are operative in the surface current multiplication as are found in the body avalanche breakdown of silicon.[21] The latter observation may be considered evidence that avalanche multiplication is operative at the surface and that the electric field at the surface in these cases is larger than in the bulk junction.

We may now consider again, briefly, the behavior of the alternating current conductance shown in Fig. 2. It has been shown above that in "wet" ambients it takes a considerable applied voltage (10 volts or more) before the inversion layer collects all the saturation current, i.e., before the inversion layer has a bias voltage, with respect to the bulk, of kT/q or more at all points. This lowered bias voltage was shown to be a consequence of the voltage drop near the main *p-n* junctions. Those regions of the inversion layer which have a bias voltage smaller than or approximately equal to kT/q cannot effectively contribute to the inversion layer conductance across the base region. They may in a certain sense be considered clamped to the potential of the base region. As the bias voltage is increased, an increasing proportion of the inversion layer rises in potential above a few times kT/q and then can contribute to the conductance across the base. It is believed that this increase in the fraction of the inversion layer that can contribute to the conductance causes the over-all rise in measured conductance.

ACKNOWLEDGMENT

The authors wish to thank Professor Harvey Brooks for stimulating discussions of the ideas presented in this paper. The authors also want to thank Mr. L. Rubin for help in the instrumentation, Mrs. J. Newell for computing assistance, and Miss M. Keilson for help with the preparation of the manuscript.

---

[21] A. G. Chynoweth and K. G. McKay, Phys. Rev. 102, 369 (1956).

PHYSICAL REVIEW VOLUME 111, NUMBER 1 JULY 1, 1958

Two-Quantum Interaction Correction for the Ground-State Energy of the Helium Atom

MARIAN GÜNTHER
Institute of Theoretical Physics, University of Warsaw, Warsaw, Poland

(Received August 6, 1957; revised manuscript received December 9, 1957)

A "frozen" potential representing mutual two-quantum interactions of two electrons is derived starting from the simplest nonrelativistic version of quantum electrodynamics. This potential is then used for calculating an energy correction for the ^1S state of the helium atom with the help of wave functions of the Hylleraas type.

I. INTRODUCTION

A WELL-KNOWN discrepancy between the experimental and theoretical values for the ionization energy of the helium atom suggests a tentative explanation by means of an electromagnetic level shift of the ^1S state strictly analogous to the Lamb shift in hydrogen. Actually a very rough estimate shows that in this way one can get a proper order of magnitude for the shift, and some attempts have already been made to obtain even more precise numerical results.[1]

Even if the situation is not quite clear at the moment as to the exact value of the energy difference to be explained,[2] it seems worthwhile to investigate in addition to the strictly "Lamb-shift-like" terms, the contributions of other interaction patterns of the same order in *e*. As "strictly Lamb-shift-like" interaction patterns, we shall consider those interactions which are represented either by exactly the same Feynman diagrams (or, more precisely, "ladders" of such diagrams) as the ordinary Lamb shift in hydrogen [Fig. 1(a)], or else by diagrams obtained from the latter by replacing the "external" photon line (representing the Coulomb potential of the nucleus) by a photon line joining the two electron lines [Fig. 1(b)].

Interactions represented by Fig. 1(a) have already been considered by many authors. As they are expected to lead to the biggest numerical results, they have formed the basis for the first rough estimates men-

---

[1] H. E. V. Hakansson, Arkiv. Fysik 1, 555 (1950); P. K. Kabir and E. E. Salpeter, Bull. Am. Phys. Soc. Ser. II, 1, 46 (1956).

[2] Compare, e.g., a discussion concerning this by S. Chandrasekhar and G. Herzberg, Phys. Rev. 98, 1050 (1955). The situation, both from the theoretical and experimental point of view, has recently changed for the better, the energy difference to be explained by radiative corrections being reduced to only 1.4±1 cm^{-1} in the same direction as the Lamb shift in hydrogen [compare, e.g., T. Kinoshita, Phys. Rev. 105, 1490 (1957)].